Ji et al. Journal of Hematology & Oncology (2026) 19:6
https://doi.org/10.1186/s13045-025-01773-4

Journal of Hematology & Oncology

CORRESPONDENCE

Open Access

A subcellular spatial atlas illuminates the microenvironmental remodeling of perineural invasion in distal cholangiocarcinoma

Fansen Ji[1,2,3†], Hao Chen[2,3†], Huan Li[4†], Jiawei Zhang[5], Sijia Li[6], Pengfei Wang[2,3], Hao Liu[4], Cui Ge[4], Bingjun Tang[2,3*], Hongfang Yin[4*], Xuedong Wang[2,3*] and Jiahong Dong[2,3*]

Abstract

Distal cholangiocarcinoma (dCCA) arises from the distal bile duct and is anatomically embedded within the pancreatic head, adjacent to abundant autonomic nerve plexuses. This unique location renders dCCA particularly prone to perineural invasion (PNI), a pathological hallmark that contributes to its dismal prognosis. However, the spatial architecture and molecular drivers that orchestrate PNI remain poorly defined. Here, we applied Xenium subcellular resolution spatial transcriptomics platform to profile resected tumor tissues from dCCA patients stratified by PNI status pathologically. A spatially resolved atlas comprising a total of 20 cell types was generated, uncovering enrichment of Schwann cells, type 2 conventional dendritic cells (cDC2), M2-like macrophages, cancer associated fibroblasts (CAFs) and B/plasma cells in PNI-high tumors, along with depletion of exhausted $CD8^+$ T cells. Heterogeneous malignant cells in PNI-high tumors demonstrated activation of extracellular matrix remodeling and axonogenesis pathways, in line with the initial pathological classification. Spatial mapping further revealed distinct PNI-associated niches, notably matrix-producing CAFs (mCAFs)-macrophage clusters exhibiting coordinated enrichment of inflammatory and fibrotic programs. We further identified the LAMB3-DAG1 axis as a potential mediator of dCCA cells-Schwann cell interaction, while the preferential proximity of arteries to Schwann cells suggested additional microenvironmental support for nerve invasion. Collectively, our study provides a comprehensive subcellular atlas of PNI in dCCA, uncovering coordinated epithelial, stromal, and immune remodeling that drives perineural invasion. The identified biomarkers not only hold promise for patient stratification but may also guide intraoperative navigation and surgical margin determination, offering new avenues for precision therapy.

†Fansen Ji, Hao Chen and Huan Li these authors contributed equally.

*Correspondence:
Bingjun Tang
tbja03642@btch.edu.cn
Hongfang Yin
yhfa00530@btch.edu.cn
Xuedong Wang
wxda01026@btch.edu.cn
Jiahong Dong
dongjiahong@tsinghua.edu.cn

Full list of author information is available at the end of the article

Keywords dCCA, PNI, Spatial transcriptomics, TME, Schwann cells

To the editor

Distal cholangiocarcinoma (dCCA) is thought to arise from biliary epithelial cells (cholangiocytes) or from biliary tree stem/progenitor cells within peribiliary/periductal glands, occupying a unique anatomical location where the bile duct courses through the pancreatic head and lies in close proximity to dense autonomic nerve plexuses and major vascular structures [1]. This anatomic context not only complicates surgical management but also predisposes dCCA to a particularly high incidence of perineural invasion (PNI), a pathological hallmark that contributes to early recurrence and poor survival outcomes [2, 3]. Despite its clinical importance, the cellular and spatial determinants of PNI within the tumor microenvironment (TME) remain poorly understood [4, 5]. The advent of spatial transcriptomics now enables a high-resolution mapping of tissue architecture and intercellular interactions in histopathological tumor tissue slides, facilitating the dissection of spatially resolved crosstalk events and molecular mechanisms underlying PNI [6–8]. Here, we employed subcellular resolution Xenium spatial transcriptomics platform [9, 10] to delineate the TME of dCCA and uncover molecular programs associated with PNI.

We analyzed resected tumor tissues from six PNI-high and three PNI-low patients, as evaluated by the density of PNI numbers considering the PNI counts relative to tumor areas by broad certificate pathologists (Fig. 1A, Table S1). Fourteen representative cores derived from tumor tissues of nine dCCA patients were included in a tissue microarray (TMA) and subjected to spatial profiling of over 5,000 genes (Fig. 1A). By integrating immunofluorescent staining, AI-based cell segmentation, and histopathological annotation, we generated a spatially subcellular resolved atlas of dCCA with 354,982 cells (Fig. 1B). In total, 20 distinct cell types were identified (Fig. 1C–E, Fig.S1A-D), revealing substantial heterogeneity across patients (Fig. 1F). Notably, PNI-high tumors exhibited enrichment of Schwann cells, cDC2, M2-like macrophages (Mph), CAF subtypes, and B/plasma cells, accompanied by depletion of $CD8^+$ exhausted T cells ($CD8^+$ Tex) (Fig. 1G, H, Fig. S1E-I). Pathway analysis of malignant cells further indicated activation of extracellular matrix (ECM) remodeling and axonogenesis programs in the PNI-high group (Fig. 1I), consistent with the histological diagnosis of perineural infiltration (Fig. 1J, Fig. S2).

Based on integrative analysis of spatial transcriptomics clustering and histological morphology, we have identified malignant and normal cell populations within the dCCA (Fig. S3). Differential gene expression analysis revealed that PNI-high malignant cells upregulated transcripts including CLDN18, ANXA5, MUC1, and CD59, which may serve as potential molecular markers for pathological assessment and provide molecular targets that may facilitate intraoperative visualization and navigation of PNI, thereby improving surgical decision-making in dCCA. (Fig. 2A, B, Fig. S4). TCGA-CHOL samples with PNI similarly demonstrated enrichment in epithelial proliferation, ECM organization, and axon development pathways (Fig. 2C, Fig. S5A, B). Spatial neighborhood analysis further identified eight distinct niches (Fig. 2D). Niches enriched in PNI-high tumors included Perineural niche (niche 4), Angio-Remodeling Niche (niche 6), Myeloid Infla Niche (niche 7), and B/Plasma Niche (niche 2) (Fig. 2E, F), highlighting PNI-associated spatial reorganization of the TME. Importantly, Mph in PNI-high tumors exhibited elevated inflammatory programs, suggesting recruitment and activation of macrophages during neural injury [8, 11]. mCAFs also showed marked upregulation of fibrosis- and ECM-associated genes (MMP14, SULF1, CTHRC1, THBS2) (Fig. 2H), further implicating stromal remodeling in the facilitation of nerve invasion.

These findings were validated using publicly available scRNA-seq data of dCCA [5], which confirmed enrichment of inflammatory CAFs (iCAFs), mCAFs, macrophages, and neutrophils in tumor versus adjacent normal tissues (Fig. 2I, Fig. S5C-J). Ligand-receptor analysis revealed that malignant-Schwann cell interactions were mediated through the LAMB3-DAG1 axis, alongside other potential regulatory pairs such as MPZ-MPZL1 and APP-SORL1 (Fig. 2J, K, Fig. S6, Table S2, 3). Single-cell and spatial transcriptomic analyses revealed that ITGB4 was predominantly expressed by Schwann cells and malignant cells (Fig. 2L), suggesting its pivotal role in mediating tumor-nerve interactions and driving PNI [12]. Interestingly, arterial-type endothelial cells (characterized by GJA5, FBLN5, GJA4 expression) were observed to be preferentially positioned adjacent to Schwann cells (Fig. 2M), underscoring a potential role of vascular-neural proximity in reinforcing the invasive niche.

In conclusion, we present a subcellularly resolved atlas of PNI in dCCA by integrating histology and tissue architecture, spatial transcriptomics, and immune–stromal profiling. Our analysis reveals coordinated epithelial, stromal, and immune remodeling that collectively drive perineural invasion, while uncovering cellular interactions and biomarkers that may enable patient stratification, inform new targeted therapies, and guide therapeutic interventions. These insights not only advance the mechanistic understanding of PNI but also

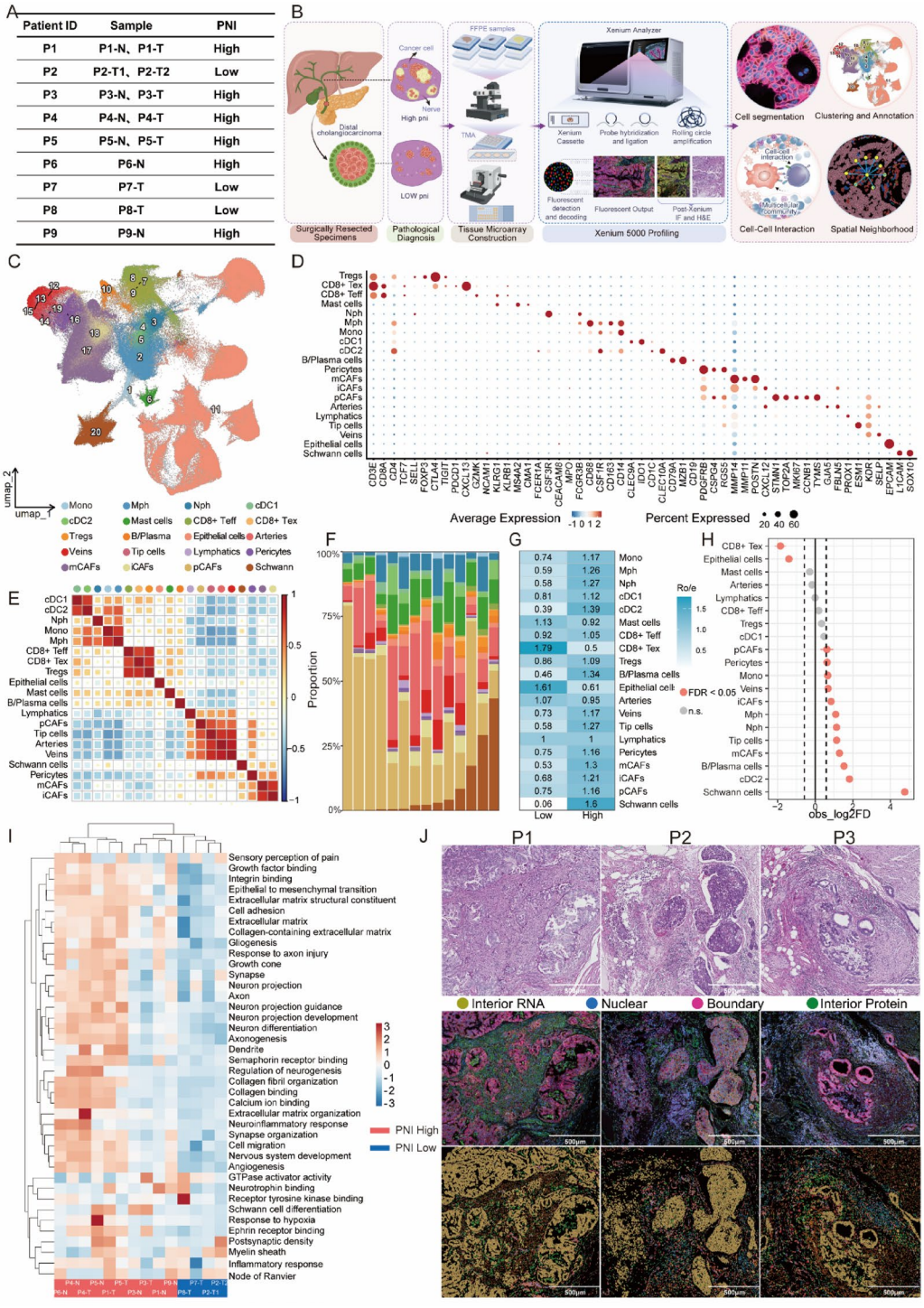

Fig. 1 Spatially resolved subcellular atlas of dCCA PNI. (**A**) Patient cohort information. (**B**) Study design and workflow for subcellular 5000-plex spatial transcriptomics profiling and integrative analysis. (**C**) UMAP visualization of all cells in Xenium 5000 data. (**D**) Dot plot showing the expression of canonical marker genes across different cell types. (**E**) Gene expression correlation matrix between cell types. (**F**) Stacked barplot of relative proportions of different cell types across all samples. (**G**) Ro/e heatmap of different cell types between PNI high and low samples. (**H**) scProportion test showing significant changes in cluster composition between tumor and adjacent normal tissues. (**I**) Heatmap of Gene Set Variation Analysis (GSVA) score for ECM and axon growth related signaling pathways across different samples. (**J**) Representative spatial maps of different cell types overlaid with H&E, immunofluorescence (IF) staining and cell type polygons from selected regions, illustrating the spatial organization of the TME for Patient P1, P2 and P3

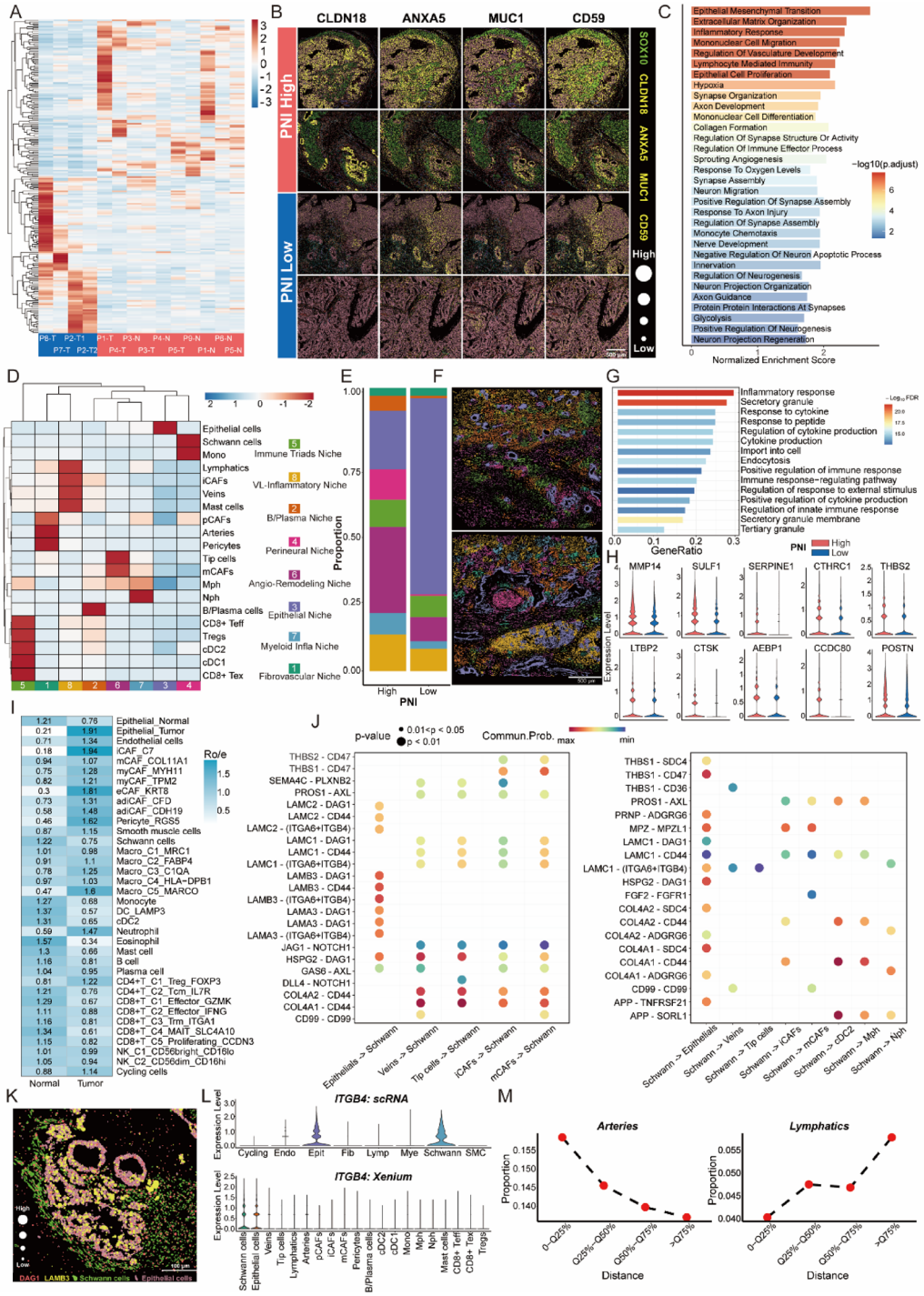

Fig. 2 Characterization of molecular and spatial reorganization in PNI-high dCCA. (**A**) Heatmap of Differentially expressed genes in malignant cells between PNI high and low group. (**B**) Spatial dot plot of transcripts (CLDN18, ANXA5, MUC1 and CD59) on representative PNI high and low group. (**C**) GO analysis of TCGA-CHOL cohort between PNI positive and negative patients highlighting ECM and axonogenesis pathways. (**D**) Heatmap of normalized cell type components between different identified spatial niches. (**E**) Stacked barplot of relative proportion of different spatial niches between PNI high and low group. (**F**) Representative image plots illustrating the distribution of different spatial niches. (**G**) Go analysis of differentially expressed genes in macrophages between PNI high and low group. (**H**) Violin plot of fibrosis and ECM-associated gene expression in mCAFs between PNI high and low group. (**I**) Ro/e heatmap of different cell types between tumor and adjacent normal samples from public scRNA-seq data of dCCA. (**J**) Cellchat Ligand-receptor bubble plot between Schwann cells and other cell types. (**K**) Representative image plot illustrating the colocalization of LAMB3 and DAG1 between Schwann cells and malignant cells. (**L**) Violin plot of ITGB4 expression in scRNA-seq data and Xenium spatial transcriptomics data of dCCA. (**M**) Scatter plot illustrating the preferential proximity of arteries to Schwann cells and separation of lymphatics from Schwann cells

hold tangible translational potential for improving clinical management of dCCA and benefit cancer patients.

Abbreviations

dCCA	Distal cholangiocarcinoma
PNI	Perineural invasion
TME	Tumor microenvironment
TMA	Tissue microarray
Mph	Macrophage
$CD8^+$ Tex	$CD8^+$ exhausted T cells
ECM	Extracellular matrix
IF	Immunofluorescence
CAFs	Cancer associated fibroblasts
mCAFs	Matrix-producing cancer-associated fibroblast
iCAFs	Inflammatory cancer-associated fibroblasts

Supplementary Information

The online version contains supplementary material available at https://doi.org/10.1186/s13045-025-01773-4.

Supplementary Material 1.

Supplementary Material 2.

Supplementary Material 3.

Supplementary Material 4.

Supplementary Material 5.

Supplementary Material 6.

Supplementary Material 7.

Supplementary Material 8.

Supplementary Material 9.

Supplementary Material 10.

Supplementary Material 11.

Acknowledgements
Not applicable.

Author contributions
Conception and design: J.D., X.W., H.Y., B.T.; Development of methodology: F.J., H.C.; Acquisition of data: F.J, H.C., H.L., B.T., H.L., C.G., J.Z., S.L., P.W.; Funding acquisition: J.D., X.W.; Data analysis and interpretation: F.J., H.C. H.L., B.T.; Figure preparation: F.J., H.C.; Writing the manuscript: F.J.; Study supervision: J.D., X.W., H.Y., B.T.; All authors read and approved the final version of the manuscript.

Funding
This study was supported by the National Science Foundation of China (92359301).

Data availability
The Xenium spatial datasets generated and/or analysed during the current study are available from [https://figshare.com/articles/dataset/Spatially_resolved_profiling_of_human_distal_cholangiocarcinoma_tissues_with_low_high_neural_invasion_status/30193333]. The scRNA-seq data supports the findings of this study are available from (https://doi.org/10.57760/sciencedb.18768) and have been previously described in the literature (PMID: 40148311) [5].

Declarations

Ethics approval and consent to participate
All experiments were performed in accordance with the approved protocol and other relevant guidelines and regulations by the Ethics Committee of Beijing Tsinghua Changgung Hospital, Tsinghua University (Approval No. 23562-0-01).

Consent for publication
Not applicable.

Competing interests
The authors declare no competing interests.

Author details
[1]Tsinghua-Peking Center for Life Sciences, Beijing, China
[2]School of Clinical Medicine, Tsinghua University, Beijing 102218, China
[3]Hepatopancreatobiliary Centre, Beijing Tsinghua Changgung Hospital, Tsinghua University, Beijing 102218, China
[4]Department of Pathology, Beijing Tsinghua Changgung Hospital, Tsinghua University, Beijing 102218, China
[5]Health Management Center, Beijing Jishuitan Hospital, Capital Medical University, Beijing 100035, China
[6]Cancer Center, Beijing Tsinghua Changgung Hospital, Tsinghua University, Beijing 102218, China

Received: 1 October 2025 / Accepted: 2 December 2025
Published online: 08 January 2026

References

1. Ilyas SI, Gores GJ. Pathogenesis, diagnosis, and management of cholangiocarcinoma. Gastroenterology. 2013;145:1215–29. https://doi.org/10.1053/j.gastro.2013.10.013.
2. Montal R, Sia D, Montironi C, Leow WQ, Esteban-Fabró R, Pinyol R, et al. Molecular classification and therapeutic targets in extrahepatic cholangiocarcinoma. J Hepatol. 2020;73:315–27. https://doi.org/10.1016/j.jhep.2020.03.008.
3. Brindley PJ, Bachini M, Ilyas SI, Khan SA, Loukas A, Sirica AE, et al. Cholangiocarcinoma Nat Rev Dis Primers Nat Publishing Group. 2021;7:1–17. https://doi.org/10.1038/s41572-021-00300-2.
4. Liu C, Wang X, Liu E, Zong Y, Yu W, Jiang Y, et al. Deciphering cholangiocarcinoma heterogeneity and specific progenitor cell niche of extrahepatic cholangiocarcinoma at single-cell resolution. J Hematol Oncol. 2025;18:66. https://doi.org/10.1186/s13045-025-01716-z.
5. Zu Z, Zhang C, Shi J, Chen K, Tang H, Hu K, et al. Single-cell analysis reveals that GFAP + dedifferentiated Schwann cells promote tumor progress in PNI-positive distal cholangiocarcinoma via lactate/HMGB1 axis. Cell Death Dis. 2025;16:215. https://doi.org/10.1038/s41419-025-07543-x.
6. Liu Y, Sinjab A, Min J, Han G, Paradiso F, Zhang Y, et al. Conserved spatial subtypes and cellular neighborhoods of cancer-associated fibroblasts revealed by single-cell spatial multi-omics. Cancer Cell. 2025;43:905-924.e6. https://doi.org/10.1016/j.ccell.2025.03.004.
7. Chang J, Lu J, Liu Q, Xiang T, Zhang S, Yi Y, et al. Single-cell multi-stage spatial evolutional map of esophageal carcinogenesis. Cancer Cell. 2025;43:380-397.e7. https://doi.org/10.1016/j.ccell.2025.02.009.
8. Chen M-M, Gao Q, Ning H, Chen K, Gao Y, Yu M, et al. Integrated single-cell and spatial transcriptomics uncover distinct cellular subtypes involved in neural invasion in pancreatic cancer. Cancer Cell. 2025;43:1656-1676.e10. https://doi.org/10.1016/j.ccell.2025.06.020.
9. Janesick A, Shelansky R, Gottscho AD, Wagner F, Williams SR, Rouault M, et al. High resolution mapping of the tumor microenvironment using integrated single-cell, spatial and in situ analysis. Nat Commun. 2023;14:8353. https://doi.org/10.1038/s41467-023-43458-x.
10. de Oliveira MF, Romero JP, Chung M, Williams SR, Gottscho AD, Gupta A, et al. High-definition Spatial transcriptomic profiling of immune cell populations in colorectal cancer. Nat Genet Nat Publishing Group. 2025;57:1512–23. https://doi.org/10.1038/s41588-025-02193-3.
11. Willis EF, MacDonald KPA, Nguyen QH, Garrido AL, Gillespie ER, Harley SBR, et al. Repopulating microglia promote brain repair in an IL-6-dependent manner. Cell. 2020;180:833-846.e16. https://doi.org/10.1016/j.cell.2020.02.013.

12. Liu Y, Han G, Feng K, Lin X, Zhong W, Liu Y, et al. ITGA5-expressing tumor cells interact with Schwann cells to drive nerve growth factor-mediated immunosuppression of NK cells. Mol Ther. 2025. https://doi.org/10.1016/j.ymthe.2025.07.043.

Publisher's note